Antarctic Sea Ice Area in CMIP6

Lettie A. Roach[1], Jakob Dörr[2], Caroline R. Holmes[3], François Massonnet[4], Edward W. Blockley[5], Dirk Notz[6,2], Thomas Rackow[7], Marilyn N. Raphael[8], Siobhan O'Farrell[9], David A. Bailey[10], Cecilia M. Bitz[1]

[1]Atmospheric Sciences, University of Washington, Seattle, WA, United States
[2]Max Planck Institute for Meteorology, Hamburg, Germany
[3]British Antarctic Survey, Cambridge, United Kingdom
[4]Georges Lemaitre Center for Earth and Climate Research, Earth and Life Institute, Université catholique de Louvain, Louvain-la-Neuve, Belgium
[5]Met Office Hadley Centre, Exeter, United Kingdom
[6]Earth System Research and Sustainability (CEN), University of Hamburg, Hamburg, Germany
[7]Alfred Wegener Institute, Helmholtz Centre for Polar and Marine Research, Climate Dynamics, Bremerhaven, Germany
[8]Department of Geography, University of California Los Angeles, CA, United States
[9]CSIRO Oceans and Atmosphere, Aspendale, Victoria, Australia
[10]Climate and Global Dynamics Laboratory, National Center for Atmospheric Research, Boulder, CO, United States

Key Points:

- CMIP6-mean Antarctic sea ice area is close to observations but inter-model spread remains substantial.
- We find modest improvements in the simulation of sea ice area and concentration compared to CMIP5.
- Most CMIP6 models simulate sea ice losses and stronger-than-observed GMST trends over 1979-2018.

Corresponding author: Lettie Roach, `lroach@uw.edu`

Abstract

Fully-coupled climate models have long shown a wide range of Antarctic sea ice states and evolution over the satellite era. Here, we present a high-level evaluation of Antarctic sea ice in 40 models from the most recent phase of the Coupled Model Intercomparison Project (CMIP6). Many models capture key characteristics of the mean seasonal cycle of sea ice area (SIA), but some simulate implausible historical mean states compared to satellite observations, leading to large inter-model spread. Summer SIA is consistently biased low across the ensemble. Compared to the previous model generation (CMIP5), the inter-model spread in winter and summer SIA has reduced and the regional distribution of sea ice concentration has improved. Over 1979-2018, many models simulate strong negative trends in SIA concurrently with stronger-than-observed trends in global mean surface temperature (GMST). By the end of the 21st century, models project clear differences in sea ice between forcing scenarios.

Plain Language Summary

Coupled climate models are complex computer programs that simulate the interaction of the atmosphere, ocean, land surface and cryosphere. An important feature of the Southern Ocean is its sea ice cover, which typically expands in winter to cover an area comparable to that of Russia. Climate models have shown very different amounts of Antarctic sea ice coverage and very different trajectories of sea ice change in response to expected greenhouse gas emissions. This year, new coupled climate models released under the Coupled Model Intercomparison Project (CMIP6) will form the basis of the next IPCC assessment report. Here, we compare output from those models to satellite observations of the areal coverage of sea ice. As a whole, the models successfully capture some elements of the observed seasonal cycle of sea ice, but under-estimate the summer minimum sea ice area. Compared to results from the previous model generation (CMIP5), the range across models has reduced and the location of sea ice agrees better with observations. Models project sea ice loss over the 21st century in all scenarios, but confidence in the rate of loss is limited as most models show stronger global warming trends than observed over the recent historical period.

1 Introduction

Antarctic sea ice area increases sixfold across the austral autumn and winter months in one of the largest seasonal area changes of any surface type on Earth. At the interface between ocean and atmosphere, the sea ice cover determines fluxes of heat, mass and momentum between these two fluids. Its presence also influences surface albedo, oceanic circulation (Pellichero et al., 2018) and the vulnerability of ice sheets to open ocean forcing (Massom et al., 2018). While Arctic sea ice has clearly decreased over the now-40-year multichannel passive-microwave satellite record, the areal extent of Antarctic sea ice shows a small positive trend over 1979-2018 (Parkinson, 2019). The increase between 2000 and 2014 was several times larger than the increase between 1979 and 1999 (Meehl et al., 2019), but was followed by sudden decreases in recent years, such that the 2017 and 2018 yearly averages were the lowest for the whole 1979-2018 record (Parkinson, 2019). A variety of mechanisms have been proposed for the increase (J. Zhang, 2007; P. R. Holland & Kwok, 2012; Haumann et al., 2014; Ferreira et al., 2015; Purich et al., 2016; Armour et al., 2016; Pauling et al., 2017) and the decrease (Meehl et al., 2019; Schlosser et al., 2018; Stuecker et al., 2017; Wang et al., 2019), but neither is well-understood.

Global coupled climate models can aid our understanding of such climate system variability and provide projections of future climate change. By providing a common model experiment protocol, the Coupled Model Intercomparison Project (CMIP) permits evaluation of climate models developed by 40 or so modelling groups worldwide. As sea ice responds to changes in the atmosphere and ocean, it is often used as a climate diagnostic. Yet despite advances in climate modelling capabilities over recent decades, simulation of Antarctic sea ice has remained a fundamental problem for state-of-the-art climate models (Turner et al., 2013; Zunz et al., 2013; Shu et al., 2015; Rosenblum & Eisenman, 2017; Roach et al., 2018; Holmes et al., 2019). The Intergovernmental Panel on Climate Change (IPCC) Fifth Assessment Report (AR5) concluded that there is 'low confidence' in climate model projections for Antarctic sea ice due to "the wide inter-model spread and the inability of almost all of the available models to reproduce the mean annual cycle, interannual variability and overall increase of the Antarctic sea ice areal coverage observed during the satellite era" (Collins et al., 2013). Similarly, the recent IPCC Special Report on the Oceans and Cryosphere in a Changing Climate found 'low confidence' in model ability to explain changes in observed Antarctic sea ice cover (Meredith et al., 2019).

Here we present an initial, high-level evaluation of Antarctic sea ice simulated by models in the sixth phase of the Coupled Model Intercomparison Project (CMIP6, Eyring et al., 2016). We focus on the areal coverage of sea ice, as this quantity can be readily obtained from satellite microwave passive radiometers. We examine the historical mean, inter-annual variability and trends in sea ice areal coverage, and leave investigation of the processes driving any particular biases to future studies.

2 Methods

The Sea Ice Model Intercomparison Project (SIMIP, Notz et al., 2016) coordinated an evaluation of Arctic sea ice in CMIP6 and established a number of community best practices (SIMIP Community, 2019). In this study, to aid comparison with Arctic results, we adopt similar approaches and diagnostics. Following SIMIP Community (2019), rather than sea ice extent, we principally consider sea ice area (SIA), computed by multiplying sea ice concentration (SIC) with individual grid-cell areas and then summing over the Southern Hemisphere. Here we also include consideration of SIC in the Supplementary Material and for calculation of the integrated ice area error (IIAE). The IIAE, adapted from the extent-based integrated ice-edge error metric (IIEE, Goessling et al., 2016), describes the area of sea ice on which models and observations disagree (Roach et al., 2018). It is the sum of SIA overestimated (O) and underestimated (U),

$$\mathrm{IIAE} = O + U, \tag{1}$$

with

$$O = \int_A \max(c_m - c_o, 0)\delta A \tag{2}$$

and

$$U = \int_A \max(c_o - c_m, 0)\delta A, \tag{3}$$

where A is the area of interest, c_m is the simulated SIC for each model and c_o is the observed SIC on a common grid. For this computation, we interpolate all data to a regular 1 degree grid, following Roach et al. (2018).

SIA from satellite observations is calculated from daily data on native grids and then averaged for each month. To sample uncertainty in retrieval algorithms (Ivanova et al., 2014), we use three observational records of SIC: OSI SAF (Lavergne et al., 2019), NASA-Team (Cavalieri et al., 1997) and Bootstrap (Comiso et al., 1997). Differences between the three observational products are greatest at the Southern Hemisphere winter maximum and the observational spread in the Antarctic is greater than in the Arctic (Fig. 1), with the lowest year-round SIA coming from the NASA-Team product. To sample uncertainty in observational products for global mean surface temperatures, we use the mean of four—Berkeley (Rohde et al., 2013), NOAA globaltemp v5.0.0 (Vose et al., 2012), GISTEMPv4 (GISTEMP Team, 2019; Lenssen et al., 2019) and HadCRUT4.6.0.0 (Morice et al., 2012)—following SIMIP Community (2019).

We use the period 1979-2014 in Sec. 3.1-3.2 to take advantage of the higher number of CMIP6 models available from the historical experiments that end in 2014, resulting in 40 CMIP6 models for comparison to 19 CMIP3 models and 38 CMIP5 models (Table S1-2). Due to the recent variability in observed Antarctic sea ice, in Subsec. 3.3 we consider trends over 1979-2018, extending the historical experiments with the ScenarioMIP experiments (O'Neill et al., 2016) where available. For this we use the SSP2-4.5 experiments, resulting in 28 CMIP6 models for Sec. 3.3, as these have the largest number of participating models, and scenarios are almost identical until 2020 (Riahi et al., 2017).

So as not to give extra weight to models providing multiple ensemble members, and for consistency with both SIMIP Community (2019) and the sea-ice analysis in IPCC AR5 (TS.SM.7.2, Stocker et al., 2013), we generally consider the first ensemble member for each ensemble. We refer to the 'CMIPx r1-ensemble' as having one ensemble member from each contributing model, and refer to individual ensembles as being the contributions from each CMIP model. All available members from individual ensembles are used only to calculate internal variability in mean sea ice area in Subsec. 3.1 and to show internal variability in sea ice area trends in Subsec. 3.3. Models are weighted equally although they may share components, a statistical limitation common to CMIP studies. Similarly, individual model ensembles are treated equally here, although methods of ensemble generation vary (c.f. Golaz et al., 2019; Danabasoglu et al., 2020). We do not demarcate individual models and observations in the main body of this paper; additional figures showing key metrics for individual models are included in the Supplementary Material.

3 Results

3.1 Mean state (1979-2014)

Fig. 1a shows the 1979-2014 mean seasonal cycle in Antarctic SIA from the CMIP6-r1 ensemble. The multi-model mean is lower than the three observational products all year, with the difference from the lowest observational product ranging between 0.4 million km^2 in December and 1.4 million km^2 in May. Two models show a very clear low bias year round, having a lower SIA in winter than many models in summer. There is substantial inter-model spread in Antarctic SIA across the ensemble. Relative to the multi-model mean values, the inter-model standard deviation in Antarctic SIA is more than twice that in the Arctic in corresponding months, and is particularly large in austral summer. In spite of the inter-model variance in mean SIA values, all models but one capture the asymmetry in the timing of the Antarctic SIA seasonal cycle, with five months retreat and seven months growth, when considering monthly data in the 1979-2014 mean.

To evaluate CMIP6 simulations in September and February, the typical maximum and minimum months of the seasonal cycle, we consider both the CMIP6 r1-ensemble as a whole (Fig. 2a-b) and agreement of individual models (Fig. S1a-b). Estimates of internal variability vary by model and we cannot judge which is most realistic, so rather than aggregating them in Fig. 2a-b, we show all estimates individually in Fig. S1a-b. The three observational products fall within the interquartile range of the CMIP6 r1-ensemble in September, indicating some consistency between the ensemble and observations (Fig. 2a). In February, the entire interquartile range is below the observations: a consistent underestimation of summer SIA (Fig. 2b). These conclusions hold when accounting for internal variability (Fig. S1a-b). As in SIMIP Community (2019), we describe individual models as being consistent with observations if the 1979-2014 mean plus or minus our estimate of internal variability falls within the observed range. Internal variability is estimated as two standard deviations across individual model ensembles with three or more ensemble members and correcting for small sample size, following SIMIP Community (2019), or two standard deviations of the corresponding pre-industrial experiment in other cases. Where both calculations are possible, estimates are generally similar (Fig. S1a-b). Using whichever is the larger estimate, 26 of the 40 CMIP6 models are consistent with observations in September and 16 out of 40 in February (Fig. S1a-b). Models may achieve consistency with observations by overestimating simulated Antarctic SIA variability, see Sec. 3.2.

Next, we consider Antarctic SIA simulated in CMIP6 relative to two previous generations (Fig. 2a-b). Comparisons between generations are unlikely be affected by internal variability, as the probability of choosing an ensemble member that is biased in any particular direction for all models in a generation is low. Besides the 40 CMIP6 models and three observational products, Fig. 2a-b show the 1979-2014 mean September and February SIA for the 19 CMIP3 models and 38 CMIP5 models. The inter-model spread is large compared to the SIA values, especially in February, and especially for CMIP5, with two CMIP5 models having more than three times the February SIA in observations. Inter-model spread is lower in CMIP6 than CMIP3 and CMIP5 in February and comparable to CMIP3 in September, despite CMIP6 having twice as many models. Multi-model r1-ensemble February mean and median values are below observations for all three model generations, but are lowest for CMIP6, indicating that the low bias in summer sea ice has worsened compared to previous CMIP generations.

The regional distribution of Antarctic sea ice is highly variable across CMIP5 (M. M. Holland et al., 2017; Roach et al., 2018). Compared to figures from those papers, the spatial distribution of SIC generally appears more uniform and more similar to observations in CMIP6 (Fig. S2-S3). Several CMIP6 models retain compact summer ice cover (Fig. S3), an aspect that was particularly poorly simulated in CMIP5 (Roach et al., 2018). In Fig. 2e-f, we quantify the spatial distribution of sea ice in February and September using the integrated ice area error (IIAE) over 1979-2014. We show the IIAE relative to the Bootstrap product only; results are similar for the two other observational products. Errors are high relative to the mean SIA values in those months, particularly in February, where in CMIP6 the model-mean IIAE is 1.6 million km^2 and the model-mean SIA is 1.4 million km^2. In both February and September, the multi-model mean and median IIAE are slightly lower in CMIP6 than CMIP5. The model inter-quartile range in IIAE is similar in CMIP6 and CMIP5, but CMIP6 has fewer outliers with a very high IIAE.

Sea ice thickness is a high-level diagnostic of energy fluxes associated with atmospheric radiation bias, ocean stratification, and heat and mass transport. We show the climatology of sea ice volume per unit grid cell area (SIVOL), sometimes referred to as ‘equivalent thickness, across the CMIP6 r1-ensemble in September and February in Fig. S4-5. The cross-model standard deviation approaches 1 m around the Antarctic Peninsula, where models show the highest SIVOL values. At least a quarter of models show large areas where SIVOL is lower than 0.5 m in September (Fig. S4) despite having high SIC

(Fig. S2). Regrettably, the lack of climatological sea ice thickness observations preclude model evaluation.

3.2 Inter-annual variability (1979-2014)

Assessments of CMIP5 models concluded that models strongly over-estimated the inter-annual variance of Antarctic sea ice extent (Collins et al., 2013; Zunz et al., 2013). Over 1979-2014, observational-mean standard deviations in detrended Antarctic SIA are 0.34 million km^2 in September and 0.26 million km^2 in February. Considering individual (detrended) CMIP6-r1 models over 1979-2014, in February, they are more or less divided equally between having higher and lower inter-annual variability than observations (Fig. S1c). In September, most individual models have higher variability than observations, in some cases exceeding observations by a factor of four (Fig. S1d).

This aspect is mostly unchanged in CMIP6 from CMIP5 and CMIP3. All three model generations have higher variability than the observations in September and overlap the observations in February (Fig. 2c-d). Thus, as a whole, models continue to over-estimate inter-annual variability at the winter maximum but appear consistent with observations in terms of variability at the summer minimum over 1979-2014. However, given that the models underestimate summer sea ice area, variability as a fraction of the mean is generally higher in models than observations in February. This result holds over 1979-2018 despite the increase in observed variability over this longer time period (not shown).

3.3 Recent historical trends (1979-2018)

The signal of observed change in Antarctic SIA and concentration over 1979-2018 is weak (Yuan et al., 2017; Handcock & Raphael, 2019; Maksym, 2019). SIA trend magnitudes over 1979-2018 are approximately half their 1979-2014 values and vary with observational product by a factor of two (Fig. 3a-b). Assuming a 2-tailed t-test and using the 95 % confidence level as a rough indicator of statistical significance, observed 1979-2018 SIA trends are significant only during winter months (Fig. S6). A small dipole pattern of increases and decreases in SIC remains in February, but few significant trends are observed in September (Fig. S7-8).

Fig. 3a-b show the observed SIA trends compared to trends in all possible 40-year segments of the pre-industrial control runs. A wide range of trends occur in the absence of greenhouse gas and aerosol forcing. This large variability may be unrealistic, given the overestimation of interannual variability (Subsec. 3.2). As with CMIP5 (e.g. Polvani & Smith, 2013), observed SIA trends lie well within this range. The more appropriate model-observations comparison is with simulations including anthropogenic forcings similar to those observed, as shown for 1979-2018 (historical simulations extended with SSP2-4.5) in Fig. 3c-d. In this case, CMIP6 sea ice trends are only marginally consistent with observed SIA trends. The values and significance of SIA trends (Fig. S6) and regions of sea ice loss (Fig. S7-S8) vary substantially across the CMIP6 r1-ensemble.

To help explain the modelled trends, Fig. 3e shows the linear trend in annual-mean SIA as a function of the annual-mean trend in global mean surface temperature (GMST) over 1979-2018. In contrast to the Arctic (e.g., Gregory et al., 2002; Winton, 2011; Mahlstein & Knutti, 2012), in the Antarctic, the observed correlation between SIA and GMST is weak, while CMIP6 models generally simulate a strong anti-correlation but with substantial across-ensemble variance (Fig. 3e). This could suggest modelled SIA is too dependent on GMST, but equally it is possible that the observed correlation would be negative and stronger in a world with stronger GMST trends and corresponding sea ice loss. From Fig. 3e, models with strong negative trends in SIA also have positive GMST trends much greater than observations—in some cases nearly twice the observations. This suggests that at least some of the mismatch with observations may relate to model climate sensitivity, rather than processes specific to the polar regions.

3.4 21st Century Projections

Finally, we consider SIA time series from 1950 to 2100 (Fig. 4), noting that projections should be treated with caution given the model biases discussed above. Fig. 4a-b show the multi-model means from the historical and midrange emissions scenarios for the CMIP3, CMIP5 and CMIP6 r1-ensembles (SRESA1b, RCP4.5 and SSP2-4.5 respectively), as this is the scenario with the largest number of model experiments. The rate of change in SIA in February and September is similar across the three generations, but with a slightly higher rate of decline in September in CMIP6 towards the end of the century. CMIP6 has the lowest multi-model mean SIA and, in February, the smallest standard deviation across the multi-model ensemble.

Fig. 4c-d show CMIP6 SIA for the historical and three forcing scenarios: SSP1-2.6, SSP2-4.5 and SSP5-8.5. The scenario multi-model means agree until around 2040 in February and September, reflecting the close agreement of the scenarios in the initial decades

(Riahi et al., 2017) and possibly the dominant role of ozone forcing in the first half of the 21st century (Barnes et al., 2014), which is similar across scenarios (Dhomse et al., 2018). Differences between scenario multi-model means are much smaller than inter-model differences within each scenario, reflecting substantial model uncertainty. By the end of the 21st century, there is clear divergence between scenarios in both February and September SIA. In February, the 2090-2099 SSP1-2.6 multi-model mean is 29 % lower than the 1979-2014 historical multi-model mean, compared to a loss of over 90 % in SSP5-8.5. In September, the losses relative to 1979-2014 are approximately 15 % and 50 % in scenarios SSP1-2.6 and SSP5-8.5 respectively.

4 Conclusions

In this study, we evaluated sea ice simulated by models from the sixth phase of the Coupled Model Intercomparison Project (CMIP6) using the now-forty-year observational record of the areal coverage of sea ice. Sea ice thickness varies across the multi-model ensemble but cannot be evaluated due to the lack of long-term observational references. We have not explored the reasons behind changes in sea ice compared to CMIP5, which may include changes to ocean vertical mixing schemes, multi-phase cloud parametrizations, ozone forcing and increased spatial resolution, including improved bathymetry. Nor have we explored the causes for continued sea ice biases in CMIP6. These may include cloud effects (Zelinka et al., 2020; Kay et al., 2016), spatial resolution that does not permit eddies, which are understood to be highly important for representation of Southern Ocean dynamics (Hallberg & Gnanadesikan, 2006; Poulsen et al., 2018; Rackow et al., 2019), and the lack of coupled ice sheet interactions, which have relevance for the entire Antarctic climate system (Bronselaer et al., 2018; Golledge et al., 2019; Pauling et al., 2017). We anticipate that future studies will investigate these aspects.

Our analysis suggests a smaller discrepancy between models and observations than previously identified due to the extended observational record. Now with four additional years of satellite data, the observed trend in SIA has weakened and the regional signals are less clear over 1979-2018 than 1979-2014. This suggests that natural variability played a major role in the observed trend, as discussed previously (Meehl et al., 2016; L. Zhang et al., 2019), and that inability of models to reproduce a positive trend should not be used as a criterion to exclude them from projections. Models with the most negative trends in SIA are those with large trends in GMST over 1979-2018, in some cases reflecting high climate sensitivity (Zelinka et al., 2020). This suggests that the disagreement with observations in historical sea ice trends is related more to climate forcing than sea ice physics. Using the full model ensemble in future emissions scenarios, model uncertainty in SIA dominates over scenario uncertainty, but multi-model means clearly diverge for the different scenarios by the end of the 21st century.

Considering SIA and concentration, we find some modest improvements in simulated Antarctic sea ice from the 40 models available compared to previous CMIP phases. Compared to CMIP5, the regional distribution of sea ice has slightly improved and the inter-model spread in mean sea ice quantities has decreased. CMIP6 models show consistency with observations at the winter maximum in September and a greater number of models retain high-concentration summer sea ice cover than CMIP5. However, they broadly under-estimate the summer minimum SIA, more so than CMIP5. Inter-annual variability of sea ice is still generally larger than that observed over the historical period, and many individual models still simulate implausible mean SIA, resulting in a large inter-model spread substantially larger than that in the Arctic. While these issues remain, overall, results suggest that we should have moderately higher confidence in simulation of Antarctic climate in CMIP6 than previous generations.

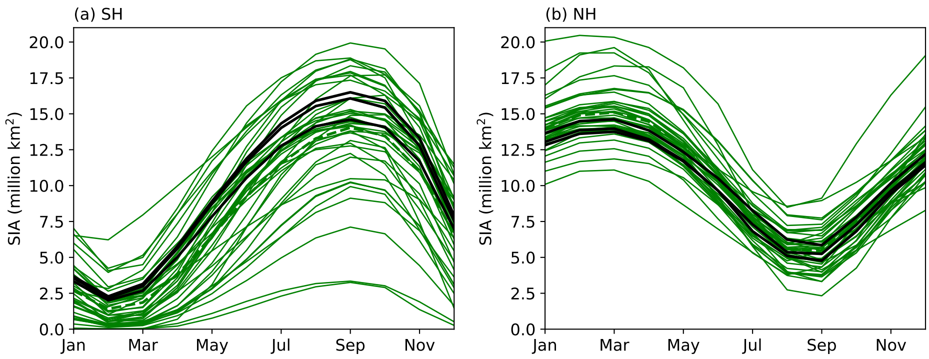

Figure 1. 1979-2014 mean seasonal cycle in SIA for the CMIP6 r1-ensemble (faint green lines), the CMIP6 multi-model mean (thick green dashed line) and three observational products (black lines) in (a) the Antarctic and (b) the Arctic.

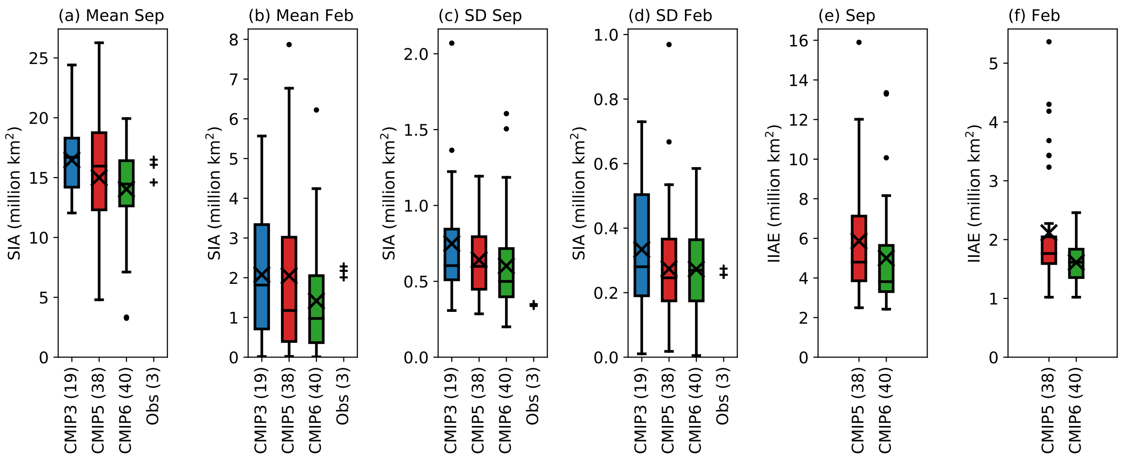

Figure 2. 1979-2014 SIA seasonal cycle statistics for the Antarctic, where boxplots contain one data point per CMIP model in the r1-ensemble. Boxes extend from the lower to upper quartile values of the data with a line at the median and a cross ('X') at the mean. Whiskers show 1.5 times the interquartile range, and data outside this range are considered outliers and shown circles. The number of models included is noted in brackets. (a) shows the September mean, (b) the February mean, (c) the September standard deviation of detrended time series, and (d) the February standard deviation of detrended time series (SD), for CMIP3, CMIP5, CMIP6 and the three observational products (marked with +). (e-f) show the integrated ice area error (IIAE) from CMIP5 and CMIP6 models in (e) February and (f) September for the 1979-2014 mean, relative to the Bootstrap observations.

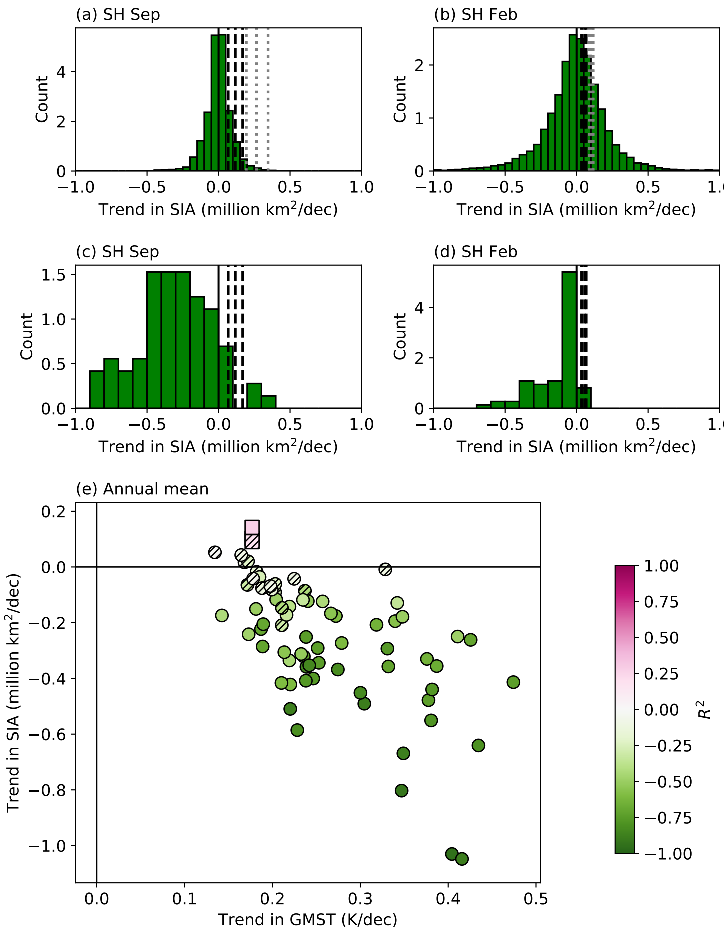

Figure 3. (a-b) Histograms of trends in Antarctic SIA in all possible 40-year segments of CMIP6 pre-industrial control runs, calculated from a least-squares linear regression and regardless of statistical significance in (a) September and (b) February. Vertical lines show trends in three observational products for (black long-dashed, -) 1979-2018 and (grey short-dashed, :) 1979-2014. (c-d) As (a-b) but for CMIP6 historical (forced) experiments over 1979-2018, using all available members from individual ensembles. (e) The linear trend in annual-mean Antarctic SIA over 1979-2018 versus the linear trend in global mean surface temperature over 1979-2018 for (circles) CMIP6 models, including all available ensemble members as individual points, and (squares) observations. The shading indicates the value of the Pearson correlation coefficient between annually-varying SIA and GMST. SIA trends that are not statistically significant at the 95 % level are hatched. Note that one model (not hatched) lies beneath the observations.

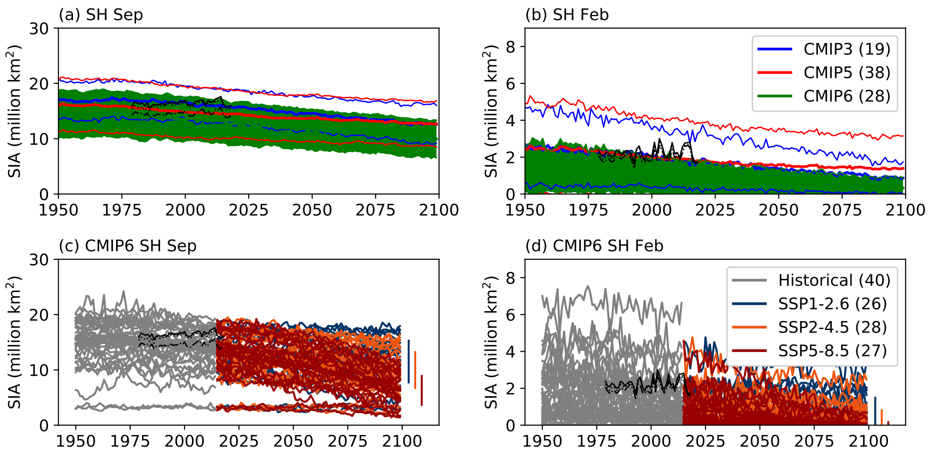

Figure 4. Antarctic SIA time series from 1950 to 2100 in February (b,d) and September (a,c). Upper plots (a,b) show the r1-ensemble-means for historical simulations and mid-range forcing scenarios: SRESA1B for CMIP3 (blue), RCP45 for CMIP5 (red) and SSP245 for CMIP6 (green). The mean plus or minus one standard deviation across the multi-model ensemble is shown as faint lines or shading corresponding to those colours. Lower plots (c,d) show historical simulations and three scenarios for the CMIP6 r1-ensemble. Three observational products are shown in black. Thick coloured lines denote multi-model means and faint lines show individual model trajectories. The number of models included in each mean is noted in brackets in the legend.

Acknowledgments

We acknowledge the World Climate Research Programme (WRCP), which, through its Working Group on Coupled Modelling, coordinated and promoted CMIP6. We thank the climate modeling groups for producing and making available their model output, the Earth System Grid Federation (ESGF) for archiving the data and providing access, and the multiple funding agencies who support CMIP6 and ESGF.

This work was inspired by the Sea Ice Model Intercomparison Project (supported by the WCRP-CliC Project) and AntClim21 (supported by the Scientific Committee on Antarctic Research, SCAR) workshops in 2019. LR would like to acknowledge travel funding from the WMO to attend both of these workshops. LR and CMB were supported by the National Science Foundation grant PLR-1643431 and National Oceanic and Atmospheric Administration grant NA18OAR4310274. JD was supported by the German Ministry for Education and Research through the project "Meereis bei +1.5 °C". CRH was supported by Natural Environment Research Council grant NE/N01829X/1. FM is a F.R.S.-FNRS Research Fellow. EB was supported by the Joint UK BEIS/Defra Met Office Hadley Centre Climate Programme (GA01101). DN was supported by the Deutsche Forschungsgemeinschaft under EXC 2037 'CLICCS - Climate, Climatic Change, and Society' Project Number: 390683824. The CESM project is supported primarily by the National Science Foundation (NSF). This material is based upon work supported by the National Center for Atmospheric Research (NCAR), which is a major facility sponsored by the NSF under Cooperative Agreement No. 1852977. We thank Doroteaciro Iovino for providing comments on an early draft of the manuscript. We are grateful to two anonymous reviewers for their assistance in improving the manuscript.

Data availability: All model output is available through `https://esgf-node.llnl.gov/projects/esgf-llnl/` (Table S1). All observational products are publicly available: OSISAF from `http://osisaf.met.no/p/ice/ice_conc_reprocessed.html` to 2015 and `http://www.osi-saf.org/?q=content/global-sea-ice-concentration-interim-climate-data-record-release-2` from 2016 onwards (Lavergne et al., 2019); NASA-Team and Bootstrap from `https://nsidc.org/data/g02202` (Meier et al., 2017); Berkeley from `http://berkeleyearth.org/data/` (Rohde et al., 2013); NOAA globaltemp v5.0.0 from `https://www.ncdc.noaa.gov/noaa-merged-land-ocean-global-surface-temperature-analysis-noaaglobaltemp-v5` (Vose et al., 2012; H.-M. Zhang et al., 2020), GISTEMPv4 from `https://data.giss.nasa.gov/gistemp/` (GISTEMP Team, 2019; Lenssen et al., 2019); and HadCRUT4.6.0.0 from `https://www.metoffice.gov.uk/hadobs/hadcrut4/` (Morice et al., 2012).

Author contributions: LR led the study. LR and JD processed the data and performed the analysis. All authors contributed to the manuscript. SO, EB and TR additionally provided model data before they were available on ESGF.

References

Armour, K. C., Marshall, J., Scott, J. R., Donohoe, A., & Newsom, E. R. (2016, 7). Southern Ocean warming delayed by circumpolar upwelling and equatorward transport. *Nature Geoscience*, *9*(7), 549–554. Retrieved from `http://www.nature.com/articles/ngeo2731` doi: 10.1038/ngeo2731

Barnes, E. A., Barnes, N. W., & Polvani, L. M. (2014). Delayed Southern Hemisphere climate change induced by stratospheric ozone recovery, as projected by the CMIP5 models. *Journal of Climate*, *27*(2), 852–867. doi: 10.1175/JCLI-D-13-00246.1

Bronselaer, B., Winton, M., Griffies, S. M., Hurlin, W. J., Rodgers, K. B., Sergienko, O. V., ... Russell, J. L. (2018). Change in future climate due to Antarctic meltwater. *Nature*, *564*(7734), 53–58. doi: 10.1038/s41586-018-0712-z

Cavalieri, D. J., Parkinson, C. L., Gloersen, P., & Zwally, H. J. (1997). *Arctic and Antarctic Sea Ice Concentrations from Multichannel Passive-Microwave Satellite Data Sets: October 1978 - September 1995 - User's Guide* (Tech. Rep.). NASA Goddard Space Flight Center Greenbelt, MD, United States.: NASA Technical Memorandum 104647.

Collins, M., Knutti, R., Arblaster, J., Dufresne, J.-L. L., Fichefet, T., Friedlingstein, P., ... Wehner, M. (2013). Long-term Climate Change: Projections, Commitments and Irreversibility Pages 1029 to 1076. In Intergovernmental Panel on Climate Change (Ed.), *Climate Change 2013 - The Physical Science Basis* (pp. 1029–1136). Cambridge: Cambridge University Press. Retrieved from `https://www.cambridge.org/core/product/identifier/CBO9781107415324A032/type/book_parthttp://www.climatechange2013.org` doi: 10.1017/CBO9781107415324.024

Comiso, J. C., Cavalieri, D. J., Parkinson, C. L., & Gloersen, P. (1997, 6). Passive microwave algorithms for sea ice concentration: A comparison of two techniques. *Remote Sensing of Environment*, *60*(3), 357–384. Retrieved from `http://linkinghub.elsevier.com/retrieve/pii/S0034425796002209` doi: 10.1016/S0034-4257(96)00220-9

Danabasoglu, G., Lamarque, J., Bacmeister, J., Bailey, D., DuVivier, A., Edwards, J., ... Strand, W. (2020). The Community Earth System Model version 2 (CESM2). *Journal of Advances in Modeling Earth Systems*, *2*, 1–35. doi:

10.1029/2019ms001916

Dhomse, S. S., Kinnison, D., Chipperfield, M. P., Salawitch, R. J., Cionni, I., Hegglin, M. I., … Zeng, G. (2018). Estimates of ozone return dates from Chemistry-Climate Model Initiative simulations. *Atmospheric Chemistry and Physics*, *18*(11), 8409–8438. doi: 10.5194/acp-18-8409-2018

Eyring, V., Bony, S., Meehl, G. A., Senior, C. A., Stevens, B., Stouffer, R. J., & Taylor, K. E. (2016, 5). Overview of the Coupled Model Intercomparison Project Phase 6 (CMIP6) experimental design and organization. *Geoscientific Model Development*, *9*(5), 1937–1958. Retrieved from http://www.geosci-model-dev.net/9/1937/2016/ doi: 10.5194/gmd-9-1937-2016

Ferreira, D., Marshall, J., Bitz, C. M., Solomon, S., & Plumb, A. (2015, 2). Antarctic Ocean and Sea Ice Response to Ozone Depletion: A Two-Time-Scale Problem. *Journal of Climate*, *28*(3), 1206–1226. Retrieved from http://journals.ametsoc.org/doi/10.1175/JCLI-D-14-00313.1 doi: 10.1175/JCLI-D-14-00313.1

GISTEMP Team. (2019). *GISS Surface Temperature Analysis (GISTEMP), version 4.* NASA Goddard Institute for Space Studies [date accessed: 12/2019]. Retrieved from https://data.giss.nasa.gov/gistemp/

Goessling, H. F., Tietsche, S., Day, J. J., Hawkins, E., & Jung, T. (2016, 2). Predictability of the Arctic sea ice edge. *Geophysical Research Letters*, *43*(4), 1642–1650. Retrieved from http://dx.doi.org/10.1002/2015GL067232http://doi.wiley.com/10.1002/2015GL067232 doi: 10.1002/2015GL067232

Golaz, J. C., Caldwell, P. M., Van Roekel, L. P., Petersen, M. R., Tang, Q., Wolfe, J. D., … Zhu, Q. (2019). The DOE E3SM Coupled Model Version 1: Overview and Evaluation at Standard Resolution. *Journal of Advances in Modeling Earth Systems*, *11*(7), 2089–2129. doi: 10.1029/2018MS001603

Golledge, N. R., Keller, E. D., Gomez, N., Naughten, K. A., Bernales, J., Trusel, L. D., & Edwards, T. L. (2019). Global environmental consequences of twenty-first-century ice-sheet melt. *Nature*, *566*(7742), 65–72. Retrieved from http://dx.doi.org/10.1038/s41586-019-0889-9 doi: 10.1038/s41586-019-0889-9

Gregory, J. M., Stott, P. A., Cresswell, D. J., Rayner, N. A., Gordon, C., & Sexton, D. M. H. (2002). Recent and future changes in Arctic sea ice simulated by the HadCM3 AOGCM. *Geophysical Research Letters*, *29*(24), 28–1. doi: 10.1029/2001gl014575

Hallberg, R., & Gnanadesikan, A. (2006). The role of eddies in determining the structure and response of the wind-driven Southern hemisphere overturning: Results from the Modeling Eddies in the Southern Ocean (MESO) project. *Journal of Physical Oceanography*, *36*(12), 2232–2252. doi: 10.1175/JPO2980.1

Handcock, M. S., & Raphael, M. N. (2019). Modeling the annual cycle of daily Antarctic sea ice extent. *The Cryosphere Discussions*, 1–19. Retrieved from `https://doi.org/10.5194/tc-2019-203` doi: 10.5194/tc-2019-203

Haumann, F. A., Notz, D., & Schmidt, H. (2014, 12). Anthropogenic influence on recent circulation-driven Antarctic sea ice changes. *Geophysical Research Letters*, *41*(23), 8429–8437. Retrieved from `http://doi.wiley.com/10.1002/2014GL061659` doi: 10.1002/2014GL061659

Holland, M. M., Landrum, L., Kostov, Y., & Marshall, J. (2017). Sensitivity of Antarctic sea ice to the Southern Annular Mode in coupled climate models. *Climate Dynamics*, *49*(5-6), 1813–1831. doi: 10.1007/s00382-016-3424-9

Holland, P. R., & Kwok, R. (2012, 12). Wind-driven trends in Antarctic sea-ice drift. *Nature Geoscience*, *5*(12), 872–875. Retrieved from `http://www.nature.com/articles/ngeo1627` doi: 10.1038/ngeo1627

Holmes, C., Holland, P., & Bracegirdle, T. (2019, 4). Compensating Biases and a Noteworthy Success in the CMIP5 Representation of Antarctic Sea Ice Processes. *Geophysical Research Letters*, *46*(8), 4299–4307. Retrieved from `https://onlinelibrary.wiley.com/doi/abs/10.1029/2018GL081796` doi: 10.1029/2018GL081796

Ivanova, N., Johannessen, O. M., Pedersen, L. T., & Tonboe, R. T. (2014, 11). Retrieval of Arctic sea ice parameters by satellite passive microwave sensors: A comparison of eleven sea ice concentration algorithms. *IEEE Transactions on Geoscience and Remote Sensing*, *52*(11), 7233–7246. Retrieved from `http://ieeexplore.ieee.org/document/6782670/` doi: 10.1109/TGRS.2014.2310136

Kay, J. E., Wall, C., Yettella, V., Medeiros, B., Hannay, C., Caldwell, P., & Bitz, C.

(2016, 6). Global Climate Impacts of Fixing the Southern Ocean Shortwave Radiation Bias in the Community Earth System Model (CESM). *Journal of Climate*, *29*(12), 4617–4636. Retrieved from `http://journals.ametsoc.org/doi/10.1175/JCLI-D-15-0358.1` doi: 10.1175/JCLI-D-15-0358.1

Lavergne, T., Sørensen, A. M., Kern, S., Tonboe, R., Notz, D., Aaboe, S., … Pedersen, L. T. (2019). Version 2 of the EUMETSAT OSI SAF and ESA CCI sea-ice concentration climate data records. *The Cryosphere*, *13*, 49–78. doi: 10.5194/tc-13-49-2019

Lenssen, N. J., Schmidt, G. A., Hansen, J. E., Menne, M. J., Persin, A., Ruedy, R., & Zyss, D. (2019). Improvements in the GISTEMP Uncertainty Model. *Journal of Geophysical Research: Atmospheres*, *124*(12), 6307–6326. doi: 10.1029/2018JD029522

Mahlstein, I., & Knutti, R. (2012). September Arctic sea ice predicted to disappear near 2°C global warming above present. *Journal of Geophysical Research Atmospheres*, *117*(6), 1–11. doi: 10.1029/2011JD016709

Maksym, T. (2019, 1). Arctic and Antarctic Sea Ice Change: Contrasts, Commonalities, and Causes. *Annual Review of Marine Science*, *11*(1), 187–213. Retrieved from `https://www.annualreviews.org/doi/10.1146/annurev-marine-010816-060610` doi: 10.1146/annurev-marine-010816-060610

Massom, R. A., Scambos, T. A., Bennetts, L. G., Reid, P., Squire, V. A., & Stammerjohn, S. E. (2018, 6). Antarctic ice shelf disintegration triggered by sea ice loss and ocean swell. *Nature*, *558*(7710), 383–389. Retrieved from `http://www.nature.com/articles/s41586-018-0212-1` doi: 10.1038/s41586-018-0212-1

Meehl, G. A., Arblaster, J. M., Bitz, C. M., Chung, C. T. Y., & Teng, H. (2016, 8). Antarctic sea-ice expansion between 2000 and 2014 driven by tropical Pacific decadal climate variability. *Nature Geoscience*, *9*(8), 590–595. Retrieved from `http://dx.doi.org/10.1038/ngeo2751http://www.nature.com/articles/ngeo2751` doi: 10.1038/ngeo2751

Meehl, G. A., Arblaster, J. M., Chung, C. T. Y., Holland, M. M., DuVivier, A., Thompson, L., … Bitz, C. M. (2019, 12). Sustained ocean changes contributed to sudden Antarctic sea ice retreat in late 2016. *Nature Communications*, *10*(1), 14. Retrieved from `http://www.nature.com/articles/`

s41467-018-07865-9 doi: 10.1038/s41467-018-07865-9

Meier, W. N., Fetterer, F., Savoie, M., Mallory, S., Duerr, R., & Stroeve, J. (2017). *NOAA/NSIDC Climate Data Record of Passive Microwave Sea Ice Concentration, Version 3. [NASA Team and Bootstrap variables].* NSIDC: National Snow and Ice Data Center, Boulder, Colorado USA [date accessed: 12/2019]. Retrieved from https://doi.org/10.7265/N59P2ZTG

Meredith, M., Sommerkorn, M., Cassotta, S., Derksen, C., Ekaykin, A., Hollowed, A., ... Schuur, A. (2019). Polar regions. In H.-O. Pörtner et al. (Eds.), *Ipcc special report on the ocean and cryosphere in a changing climate.* in press.

Morice, C. P., Kennedy, J. J., Rayner, N. A., & Jones, P. D. (2012). Quantifying uncertainties in global and regional temperature change using an ensemble of observational estimates: The HadCRUT4 data set. *Journal of Geophysical Research Atmospheres*, *117*(8), 1–22. doi: 10.1029/2011JD017187

Notz, D., Jahn, A., Holland, M., Hunke, E., Massonnet, F., Stroeve, J., ... Vancoppenolle, M. (2016, 9). The CMIP6 Sea-Ice Model Intercomparison Project (SIMIP): understanding sea ice through climate-model simulations. *Geoscientific Model Development*, *9*(9), 3427–3446. Retrieved from https://www.geosci-model-dev.net/9/3427/2016/ doi: 10.5194/gmd-9-3427-2016

O'Neill, B. C., Tebaldi, C., Van Vuuren, D. P., Eyring, V., Friedlingstein, P., Hurtt, G., ... Sanderson, B. M. (2016). The Scenario Model Intercomparison Project (ScenarioMIP) for CMIP6. *Geoscientific Model Development*, *9*(9), 3461–3482. doi: 10.5194/gmd-9-3461-2016

Parkinson, C. L. (2019). A 40-y record reveals gradual Antarctic sea ice increases followed by decreases at rates far exceeding the rates seen in the Arctic. *Proceedings of the National Academy of Sciences of the United States of America*, *116*(29), 14414–14423. doi: 10.1073/pnas.1906556116

Pauling, A. G., Smith, I. J., Langhorne, P. J., & Bitz, C. M. (2017, 10). Time-Dependent Freshwater Input From Ice Shelves: Impacts on Antarctic Sea Ice and the Southern Ocean in an Earth System Model. *Geophysical Research Letters*, *44*(20), 454–10. Retrieved from http://doi.wiley.com/10.1002/2017GL075017 doi: 10.1002/2017GL075017

Pellichero, V., Sallée, J.-B., Chapman, C. C., & Downes, S. M. (2018, 12). The Southern Ocean meridional overturning in the sea-ice sector is driven by freshwater fluxes. *Nature Communications*, *9*(1), 1789. Retrieved from http://dx.doi.org/10.1038/s41467-018-04101-2http://www.nature.com/articles/s41467-018-04101-2 doi: 10.1038/s41467-018-04101-2

Polvani, L. M., & Smith, K. L. (2013, 6). Can natural variability explain observed Antarctic sea ice trends? New modeling evidence from CMIP5. *Geophysical Research Letters*, *40*(12), 3195–3199. Retrieved from http://doi.wiley.com/10.1002/grl.50578 doi: 10.1002/grl.50578

Poulsen, M. B., Jochum, M., & Nuterman, R. (2018, 4). Parameterized and resolved Southern Ocean eddy compensation. *Ocean Modelling*, *124*(April 2017), 1–15. Retrieved from https://doi.org/10.1016/j.ocemod.2018.01.008http://linkinghub.elsevier.com/retrieve/pii/S1463500318300258 doi: 10.1016/j.ocemod.2018.01.008

Purich, A., Cai, W., England, M. H., & Cowan, T. (2016, 2). Evidence for link between modelled trends in Antarctic sea ice and underestimated westerly wind changes. *Nature Communications*, *7*, 10409. Retrieved from http://www.nature.com/doifinder/10.1038/ncomms10409 doi: 10.1038/ncomms10409

Rackow, T., Sein, V. D., Semmler, T., Danilov, S., Koldunov, V. N., Sidorenko, D., … Jung, T. (2019). Sensitivity of deep ocean biases to horizontal resolution in prototype CMIP6 simulations with AWI-CM1.0. *Geoscientific Model Development*, *12*(7), 2635–2656. doi: 10.5194/gmd-12-2635-2019

Riahi, K., van Vuuren, D. P., Kriegler, E., Edmonds, J., O'Neill, B. C., Fujimori, S., … Tavoni, M. (2017). The Shared Socioeconomic Pathways and their energy, land use, and greenhouse gas emissions implications: An overview. *Global Environmental Change*, *42*, 153–168. doi: 10.1016/j.gloenvcha.2016.05.009

Roach, L. A., Dean, S. M., & Renwick, J. A. (2018, 1). Consistent biases in Antarctic sea ice concentration simulated by climate models. *The Cryosphere*, *12*(1), 365–383. Retrieved from https://www.the-cryosphere.net/12/365/2018/ doi: 10.5194/tc-12-365-2018

Rohde, R., Muller, R., Jacobsen, R., Perlmutter, S., & Mosher, S. (2013). Berkeley Earth Temperature Averaging Process. *Geoinformatics & Geostatistics: An Overview*, *01*(02). doi: 10.4172/2327-4581.1000103

Rosenblum, E., & Eisenman, I. (2017, 8). Sea Ice Trends in Climate Models Only

Accurate in Runs with Biased Global Warming. *Journal of Climate*, *30*(16), 6265–6278. Retrieved from `http://journals.ametsoc.org/doi/10.1175/JCLI-D-16-0455.1` doi: 10.1175/JCLI-D-16-0455.1

Schlosser, E., Haumann, F. A., & Raphael, M. N. (2018, 3). Atmospheric influences on the anomalous 2016 Antarctic sea ice decay. *The Cryosphere*, *12*(3), 1103–1119. Retrieved from `https://www.the-cryosphere.net/12/1103/2018/` doi: 10.5194/tc-12-1103-2018

Shu, Q., Song, Z., & Qiao, F. (2015, 2). Assessment of sea ice simulations in the CMIP5 models. *The Cryosphere*, *9*(1), 399–409. Retrieved from `https://www.the-cryosphere.net/9/399/2015/` doi: 10.5194/tc-9-399-2015

SIMIP Community. (2019). Arctic Sea Ice in CMIP6. *Geophysical Research Letters*, *in prep.*

Stocker, T., Qin, D., Plattner, G.-K., Alexander, L., Allen, S. K., Bindoff, N., … Xie, S.-P. (2013). Technical Summary Supplementary Material. In T. Stocker et al. (Eds.), *Climate change 2013: The physical science basis. contribution of working group i to the fifth assessment report of the intergovernmental panel on climate change.* Retrieved from `www.climatechange2013.orgwww.ipcc.ch`

Stuecker, M. F., Bitz, C. M., & Armour, K. C. (2017, 9). Conditions leading to the unprecedented low Antarctic sea ice extent during the 2016 austral spring season. *Geophysical Research Letters*, *44*(17), 9008–9019. Retrieved from `http://doi.wiley.com/10.1002/2017GL074691` doi: 10.1002/2017GL074691

Turner, J., Bracegirdle, T. J., Phillips, T., Marshall, G. J., Hosking, J. S., & Scott Hosking, J. (2013, 3). An initial assessment of Antarctic sea ice extent in the CMIP5 models. *Journal of Climate*, *26*(5), 1473–1484. Retrieved from `http://dx.doi.org/10.1175/JCLI-D-12-00068.1http://journals.ametsoc.org/doi/abs/10.1175/JCLI-D-12-00068.1` doi: 10.1175/JCLI-D-12-00068.1

Vose, R. S., Arndt, D., Banzon, V. F., Easterling, D. R., Gleason, B., Huang, B., … Wuertz, D. B. (2012). NOAA's merged land-ocean surface temperature analysis. *Bulletin of the American Meteorological Society*, *93*(11), 1677–1685. doi: 10.1175/BAMS-D-11-00241.1

Wang, Z., Turner, J., Wu, Y., & Liu, C. (2019, 9). Rapid Decline of Total Antarctic Sea Ice Extent during 201416 Controlled by Wind-Driven Sea Ice Drift. *Journal of Climate*, *32*(17), 5381–5395. Retrieved from http://journals.ametsoc.org/doi/10.1175/JCLI-D-18-0635.1 doi: 10.1175/JCLI-D-18-0635.1

Winton, M. (2011). Do climate models underestimate the sensitivity of Northern Hemisphere sea ice cover? *Journal of Climate*, *24*(15), 3924–3934. doi: 10.1175/2011JCLI4146.1

Yuan, N., Ding, M., Ludescher, J., & Bunde, A. (2017, 12). Increase of the Antarctic Sea Ice Extent is highly significant only in the Ross Sea. *Scientific Reports*, *7*(1), 41096. Retrieved from http://dx.doi.org/10.1038/srep41096http://www.nature.com/articles/srep41096 doi: 10.1038/srep41096

Zelinka, M. D., Myers, T. A., McCoy, D. T., Po-Chedley, S., Caldwell, P. M., Ceppi, P., … Taylor, K. E. (2020). Causes of Higher Climate Sensitivity in CMIP6 Models. *Geophysical Research Letters*, *47*(1), 1–12. doi: 10.1029/2019GL085782

Zhang, H.-M., Huang, B., Lawrimore, J., Menne, M., & Smith, T. M. (2020). *NOAA Global Surface Temperature Dataset (NOAAGlobalTemp), Version 4.0.* NOAA National Centers for Environmental Information [date accessed: 12/2019]. Retrieved from https://doi.org/10.7289/V5FN144H

Zhang, J. (2007). Increasing Antarctic sea ice under warming atmospheric and oceanic conditions. *Journal of Climate*, *20*(11), 2515–2529. doi: 10.1175/JCLI4136.1

Zhang, L., Delworth, T. L., Cooke, W., & Yang, X. (2019). Natural variability of Southern Ocean convection as a driver of observed climate trends. *Nature Climate Change*, *9*(1), 59–65. Retrieved from http://dx.doi.org/10.1038/s41558-018-0350-3 doi: 10.1038/s41558-018-0350-3

Zunz, V., Goosse, H., & Massonnet, F. (2013, 3). How does internal variability influence the ability of CMIP5 models to reproduce the recent trend in Southern Ocean sea ice extent? *The Cryosphere*, *7*(2), 451–468. Retrieved from https://www.the-cryosphere.net/7/451/2013/ doi: 10.5194/tc-7-451-2013